Mod Pathol 36 (2023) 100251

MODERN PATHOLOGY

USCAP UNITED STATES AND CANADIAN ACADEMY OF PATHOLOGY
Creating a Better Pathologist

Journal homepage: https://modernpathology.org/

Research Article

# Clinical and Genomic Characterization of Pancreatic Ductal Adenocarcinoma with Signet-Ring/Poorly Cohesive Cells

Michele Simbolo[a], Nicola Silvestris[b], Giuseppe Malleo[c], Andrea Mafficini[a,d], Laura Maggino[c], Alessandra Cocomazzi[d], Lisa Veghini[a], Aldo Mombello[a], Francesco Pezzini[a], Elisabetta Sereni[c], Filippo M. Martelli[a], Anastasios Gkountakos[d], Chiara Ciaparrone[d], Maria L. Piredda[d], Giuseppe Ingravallo[e], Gaetano Paolino[a], Floriana Nappo[f], Ilario G. Rapposelli[g], Luca Frassinetti[g], Luca Saragoni[h], Sara Lonardi[f], Antonio Pea[c], Salvatore Paiella[c], Matteo Fassan[i], Oronzo Brunetti[j], Sara Cingarlini[k], Roberto Salvia[c], Michele Milella[k], Vincenzo Corbo[a], Rita T. Lawlor[a,d], Aldo Scarpa[a,d], Claudio Luchini[a,d,*]

[a] *Department of Diagnostics and Public Health, Section of Pathology, University and Hospital Trust of Verona, Verona, Italy;* [b] *Medical Oncology Unit, Department of Human Pathology "G. Barresi", University of Messina, Messina, Italy;* [c] *Department of Surgery, The Pancreas Institute, University and Hospital Trust of Verona, Verona, Italy;* [d] *ARC-Net Research Center, University and Hospital Trust of Verona, Verona, Italy;* [e] *Department of Emergency and Transplantation, Pathology Section, University of Bari Medical School, Bari, Italy;* [f] *Medical Oncology 1, Veneto Institute of Oncology IOV-IRCCS, Padua, Italy;* [g] *Medical Oncology Unit, IRST IRCCS, Meldola, Italy;* [h] *Department of Pathological Anatomy, AUSL Romagna, Morgagni-Pierantoni Hospital, Forlì, Italy;* [i] *Surgical Pathology Unit, Department of Medicine (DIMED), University of Padua, and Veneto Institute of Oncology, IOV-IRCCS, Padua, Italy;* [j] *IRCCS Istituto Tumori "Giovanni Paolo II" of Bari, Vari, Italy;* [k] *Department of Medicine, Section of Oncology, University and Hospital Trust of Verona, Verona, Italy*

## ARTICLE INFO

*Article history:*
Received 12 February 2023
Revised 30 May 2023
Accepted 15 June 2023
Available online 22 June 2023

*Keywords:*
pancreatic cancer
pancreatic ductal adenocarcinoma
PDAC
poorly cohesive
signet-ring

## ABSTRACT

Signet-ring cell (SRC)/poorly cohesive cell carcinoma is an aggressive variant of pancreatic ductal adenocarcinoma (PDAC). This study aimed to clarify its clinicopathologic and molecular profiles based on a multi-institutional cohort of 20 cases.

The molecular profiles were investigated using DNA and RNA sequencing. The clinicopathologic parameters and molecular alterations were analyzed based on survival indices and using a validation/comparative cohort of 480 conventional PDAC patients.

The primary findings were as follows: (1) clinicopathologic features: SRC carcinomas are highly aggressive neoplasms with poor prognosis, and the lungs are elective metastatic sites; (2) survival analysis: a higher SRC component was indicative of poorer prognosis. In particular, the most clinically significant threshold of SRC was 80%, showing statistically significant differences in both disease-specific and disease-free survival; (3) genomic profiles: SRC carcinomas are similar to conventional PDAC with the most common alterations affecting the classic PDAC drivers *KRAS* (70% of cases), *TP53* (55%), *SMAD4* (25%), and *CDKN2A* (20%). *EGFR* alterations, *RET*::*CCDC6* fusion gene, and microsatellite instability (3 different cases, 1 alteration per case) represent novel targets for precision oncology. The occurrence of *SMAD4* mutations was associated with poorer prognosis; (4) pancreatic SRC carcinomas are genetically different from gastric SRC carcinomas: *CDH1*, the classic driver gene of gastric SRC carcinoma, is not altered in pancreatic SRC carcinoma; (5) transcriptome analysis: the cases clustered into 2 groups, one classical/exocrine-like, and the other squamous-like;

These authors contributed equally: Michele Simbolo, Nicola Silvestris, and Giuseppe Malleo.

* Corresponding author.
E-mail address: claudio.luchini@univr.it (C. Luchini).


https://doi.org/10.1016/j.modpat.2023.100251

and (6) SRC carcinoma-derived organoids can be successfully generated, and their cultures preserve the histologic and molecular features of parental SRC carcinoma.

Although pancreatic SRC carcinoma shares similarities with conventional PDAC regarding the most important genetic drivers, it also exhibits important differences. A personalized approach for patients with this tumor type should consider the clinical relevance of histologic determination of the SRC component and the presence of potentially actionable molecular targets.



## Introduction

Pancreatic cancer is the seventh leading cause of global cancer-related deaths in Western countries and is projected to become the second most common cancer worldwide in the next decade.[1–3] More than 80% of patients with pancreatic cancer are already diagnosed with locally advanced or metastatic disease and are not amenable to surgical resection with curative intent.[3] Despite some progress in chemotherapeutic strategies, the prognosis remains poor with a 5-year overall survival slightly exceeding 10%.[3,4] To improve opportunities for pancreatic cancer treatment, new therapeutic approaches are urgently required. In support of this, one of the most promising tools is the integration of histologic characterization with the molecular profile to identify potential molecular targets for precision oncology.[5]

Pancreatic ductal adenocarcinoma (PDAC) is the most common type of pancreatic cancer and accounts for greater than 90% of all pancreatic malignancies.[4] Histologically, the majority of PDAC is represented by conventional PDAC; however, the current World Health Organization (WHO) classification has also identified different PDAC variants, and each possesses a peculiar morphology and specific molecular correlates.[4,6–8] Notably, subtyping pancreatic cancer with comprehensive histomolecular profiling may help clinicians to define the best therapeutic choices and improve patient clinical outcomes.[4,6–8]

A rare and aggressive PDAC variant is represented by signet-ring cell (SRC)/poorly cohesive cell carcinoma. By definition, this histologic subtype is composed of at least 80% SRCs that appear as individually infiltrating cells with signet-ring elements possessing typical intracellular mucin vacuoles that peripherally displace the nuclei.[4] To date, very few studies have described this specific PDAC variant.[9–12] and its histomolecular profile is yet to be elucidated. Due to its low prevalence and reporting, specific treatment guidelines for this PDAC subtype do not exist, and therapeutic choices are based on the existing literature focused on pancreatic adenocarcinoma.

This study aimed to investigate the histologic and molecular features of PDAC containing SRC to provide a better comprehension of its histomolecular profiles, to determine the clinical importance of its correct identification within the diagnostic workflow, and to detect new possible targets for precision oncology.

## Materials and Methods

In 2019, an Italian multi-institutional task force that was termed the Italian rare pancreatic exocrine cancer initiative (IRaPaCa) was created with the specific aim of studying rare histotypes and variants of PDAC.[13] The study involved 21 different Italian centers with medium-to-high volumes of surgery for pancreatic cancer. This study that focused on SRC carcinoma of the pancreas was approved by the Bari Ethics Committee (date of approval: 10-01-2018, project n.242, code: 708/CE). Experiments involving organoids and clinical data extraction were approved by the Verona Ethics Committee (date of approval: September 19, 2018, project no. 1911, code: 61413, and PAD_R no. 1101 CESC). All procedures were conducted in accordance with the Good Practice Guidelines, the Declaration of Helsinki, and current laws, ethics, and regulations.

### *Acquisition of Samples and Clinical Data and Histopathologic Assessment*

A series of 1390 consecutive pancreatic resection specimens of PDAC from the leading institution (University of Verona) and the electronic database of all other involved centers were searched for SRC carcinomas. For the participating centers, both surgical resections and biopsy materials were considered. All slides of the selected tumors were finally reviewed blindly by 2 pancreatic pathologists (C.L., A.S.) to select only PDAC with an undebatable presence of SRC and to estimate the percentage of SRC. In the case of inconsistencies, they were resolved by consensus at multiheaded microscope with a third pathologist (M.F.). To further investigate the biological significance of SRC in the pancreas, PDAC with a percentage of SRC $< 80\%$ but $> 50$ were selected. Medical records and electronic databases were reviewed to obtain additional clinicopathologic data, including the available survival information. Only cases with an undebatable pancreatic origin were included, and cases with ampullary or duodenal origin were excluded from the study. Furthermore, given the histologic peculiarity of SRC that is typical for tumors of the stomach, patients with a history of gastric cancer were excluded from the study. Concomitant gastric neoplasms were excluded using imaging. All cases were extensively characterized histologically, and for each case, an area of cancer exclusively composed of SRC was selected and manually microdissected for molecular analysis.

### *Molecular Analysis*

#### *Genomic Next-Generation Sequencing*

After DNA extraction (Supplementary Methods), Next-Generation Sequencing (NGS) was performed using the SureSelectXT HS CD Glasgow Cancer Core assay (www.agilent.com), hereinafter referred to as CORE, as previously described.[14] Briefly, the assay spans 1.8 megabases of the genome and interrogates 174 genes for somatic mutations, copy number alterations, and structural rearrangements; the detail of targeted genes is reported in Supplementary Table S1. Sequencing was performed on a NextSeq 500 (Illumina) loaded with 2 captured library pools, using a high-output flow cell and $2 \times 75$ bp paired-end sequencing. CORE panel analysis started with demultiplexing performed with

FASTQ Generation v1.0.0 on the BaseSpace Sequence Hub (https://basespace.illumina.com, last accessed date September 14, 2022). Forward and reverse reads from each demultiplexed sample were aligned to the human reference genome (version hg38/GRCh38) using BWA and saved in the BAM file format.[15] BAM files were sorted, subjected to PCR duplicate removal, and indexed using biobambam2 v2.0.146 (https://gitlab.com/german.tischler/biobambam2.git; last accessed date September 14, 2022).[16] Coverage statistics were produced using samtools.[17] Microsatellite instability (MSI) was computed following the method of Papke et al,[18] and as already described.[14] Structural rearrangements were detected using the BRASS software.[19]

In addition to CORE, another NGS panel was tested on all samples for investigating the mutational status of *CDH1*, a gene of pivotal importance in gastric SRC carcinoma but not included within the CORE panel. To this aim, a custom-made NGS analysis covering all coding exons of *CDH1* gene was developed. NGS was performed on the Ion Torrent platform using 40 ng of DNA. Emulsion PCR to construct the libraries of clonal sequences was performed with the Ion Chef System, whereas sequencing was performed using the S5XL instrument (ThermoFisher Scientific). Data analysis, including variant calling, was performed by using Torrent Suite Software, version 5.1 (ThermoFisher Scientific).

Variants were classified as Benign (class 1), Likely Benign (class 2), Variant of Uncertain Significance (VUS − class 3), Likely pathogenic (class 4), and pathogenic (class 5), as per the American College of Medical Genetics and Genomics and the Association for Molecular Pathology (ACMG/AMP) recommendation.[20]

*MSI Analysis*

In the cases where targeted sequencing revealed the presence of MSI, we assessed the expression of the mismatch repair proteins, namely, MLH1 (clone: ES05; dilution 1:30; Dako), PMS2 (MRQ-28, 1:150, Cell Marque Impath Menarini), MSH2 (FE11; 1:30, Dako), and MSH6 (EP49; 1:100, Dako), using immunohistochemistry (IHC) as described elsewhere.[21] If NGS reported the presence of MSI but did not find any genetic alteration of MMR genes, a specific *MLH1* promoter methylation analysis was assessed using pyrosequencing, with the PyroMark Q96 ID, and analyzed using the PyroMark Q96 ID software (Qiagen), as already described.[20] Samples were considered hypermethylated when methylation of CpG islands was $\geq$ 14%, as per manufacturer instructions.

*Transcriptome Analysis by RNA Sequencing*

After RNA extraction (Supplementary Methods), the RNA sequencing (RNAseq) libraries were produced using the NEBNext Ultra II Directional RNA Library Prep Kit following the rRNA depletion workflow (NEB). All libraries were sequenced on an Illumina platform at 150 paired-end (Illumina). Quality check of the raw sequencing reads was performed using FastQC (v0.11.9). Novel transcripts reconstruction and gene expression quantification were carried out using Stringtie (v2.1.5). STAR-Fusion (v1.10.1) was used to identify candidate fusion transcripts, followed by FusionInspector (v2.2.1) to perform a supervised analysis of fusion predictions and for producing HTML-based fusion reports.

Counts were normalized and transformed using the "DESeq2" package for R (Foundation for Statistical Computing; https://www.r-project.org, last accessed date December 30, 2022).[22] Visualization and clustering were performed using the "ComplexHeatmap" package for R.[23] Differential expression analysis between groups was performed using the Deseq2 algorithm. A gene was considered differentially expressed if it showed an adjusted *P*-value < .05. Pancreatic cancer signatures were retrieved from studies performed by Bailey et al,[24] Collisson et al,[25] and Moffitt et al[26]; for clustering analysis, c2 and H pathways from MSigDB were adopted.[27,28] For analyzing significant up- and downregulated pathways between clusters, also applying a *z*-score normalization between clusters, the GSEA/GAGE R package was used.[29] An additional differential expression analysis using the Deseq2 algorithm, coupled with a GSEA-based approach, was also used to compare cases with and without lung metastasization.

*Additional Immunohistochemistry*

Additional IHC was performed on the 17 surgically resected specimens; it was used for further investigating the biological peculiarities of pancreatic cancer with SRC, as well as for validating transcriptome analysis. We performed IHC for the most used mucins in pancreatic pathology, also comparing their expression with the results of transcriptome analysis. Two specific markers differentially expressed between clusters A vs B, cytokeratin 17 and cytokeratin19, were also tested for further validation. IHC was performed following an already described methodology.[30] and using the following antibodies: MUC1 (clone: Ma695, source: Leica, dilution: prediluted), MUC2 (Ccp58, Novocastra, prediluted), MUC4 (CB12, Abcam, 1:3000), MUC5A5 (CLH2, Dako, 1:50), MUC6 (CLH5, Leica, prediluted), cytokeratin 17 (E3, Dako, 1:30), and cytokeratin 19 (RCK108, Dako, 1:100). The overall evaluation was made using a combined quantitative and qualitative score, as already described.[31] First, the percentage of positive cells was calculated by assigning a quantitative score, as follows: no positive cells = score 0, 1% to 25% = 1, 26% to 50% = 2, 51% to 75% = 3, and 76% to 100% = 4. Then, a qualitative evaluation was performed, assigning a score based on the staining intensity: score 0 = no staining, 1 = weak staining, 2 = moderate staining, and 3 = strong staining. Finally, the combined score was calculated by multiplying the quantitative and qualitative scores, with the final combined score ranging from 0 to 12.

*Organoid-Based Analysis*

To further investigate the biology of pancreatic cancer with SRC, an organoid-based exploratory analysis was performed. To this aim, an organoid culture was generated starting from a case of SRC-PDAC. After organoid establishment and dissociation (Supplementary Methods), DNA was extracted using DNeasy Blood and Tissue kit (Qiagen) according to the manufacturer's instruction, and analyzed with the CORE panel, as previously described. RNA extraction from organoids was performed with TRIzol (Life Technologies). TruSeq sample Prep Kit V2 (Illumina) was used to prepare sequencing libraries following the manufacturer's instructions. For RNAseq, libraries were multiplexed and sequenced with NextSeq 500 platform with paired-end reads of 101 bases with a final coverage of 30 million reads per sample. Also for organoid, pancreatic cancer signatures were retrieved from studies performed by Bailey et al[24] and Moffitt et al[26] to calculate the main PDAC transcriptome subtypes.

*Clinical/Survival Analysis*

For statistical purposes, in the context of survival analysis, we decided to analyze the present cohort of pancreatic SRC

carcinoma and a validation series of conventional PDAC as a control cohort. The main aims were (1) to understand if SRC carcinoma exhibits a different clinical behavior than conventional PDAC; (2) to investigate the potential presence of prognostic variables; (3) to verify if the WHO-based diagnostic threshold of 80% SRC exerts a clinical impact. All *P*-values are presented as hazard ratios (HR) and 95% CIs as appropriate. Statistical significance was determined using a *P*-value < .05.

For the control cohort, we selected only conventional PDAC without SRC that was resected in the same timeframe as the SRC carcinoma cohort. Specific exclusion criteria for the conventional PDAC control cohort were receipt of neoadjuvant treatment, presence of distant metastases, R2 resection, in-hospital mortality, and missing information regarding disease-specific survival (DSS) or recurrence-free survival (RFS).

For SRC carcinoma and the control cohort, data were analyzed using R.4.0.0 software (detailed in Supplementary Methods). Univariate and multivariate analyses (Cox's regression models) were conducted considering all cases and variables that included % SRC, age, sex, tumor stage, and R status, and for the SRC cohort, genomic variables including recurrent alterations and transcriptome clusters. Survival curves were constructed using the Kaplan–Meier method, and pairwise differences between groups were assessed using the log-rank test.

As a further control and to exclude possible baseline imbalances in patient characteristics between SRC carcinoma and conventional PDAC cohorts, we also performed an additional specific analysis that included propensity-score matching. Propensity scores were calculated using logistic regression modeling while accounting for age, sex, tumor stage, and R status. SRC carcinoma and conventional PDAC were paired at 1:10 based on these propensity scores using the greedy nearest-neighbor matching algorithm without replacement and a caliper size of 0.1. Standardized mean differences were estimated before and after matching to evaluate the balance of covariates, and small absolute values (<0.1) indicated a balance between the groups. The R packages "*MatchIt*" and "*cobalt*" were used.

## Results

### *Histopathologic Assessment*

Overall, 20 cases of pancreatic cancer with SRC were identified, including 16 primary surgical resections, 3 fine-needle biopsies, and an autopsy case of widespread metastatic pancreatic SRC carcinoma (pancreatic cancer with rapid and massive spread to lungs). The cases exhibited a variable proportion of SRC that is summarized in Table 1 along with their clinicopathologic features. Briefly, 11 cases satisfied the WHO definition of pancreatic adenocarcinoma with SRC and comprised at least 80% of these types of cells. The other 6 cases possessed SRC percentages ranging from 50% to 60%. Finally, the 3 biopsies included percentages of SRC ranging from 50% to 80%. Illustrative histologic representations are presented in Figure 1 and Supplementary Figure S1.

Most patients (90%) exhibited involvement of the pancreatic head. Vascular invasion and perineural infiltration were detected in all cases concerning the histologic aspects associated with aggressive biological behavior. Only 1 patient did not exhibit nodal metastasis (pN0) at the time of diagnosis. Considering only surgically resected patients and those with available survival information, 7/13 died during follow-up. Regarding patients who experienced tumor relapse/metastasis during follow-up, all patients (8/8, 100%) exhibited involvement of the lungs, and of these, the majority (5/8, 62.5%) presented with lungs as the first metastatic site.

**Table 1**
Summarizing table of the most important clinicopathologic information of this case series

| ID case | Age (y) | Sex | Main histology | Secondary histology | Specimen | Site | Size (cm) | pTNM | Stage | LVI | PNI | R status | Survival (months/event) |
|---|---|---|---|---|---|---|---|---|---|---|---|---|---|
| 1 | 58 | M | SR 100% | NA | AUT | H-B | 5.5 | T4N2M1 | IV | Yes | Yes | NA | DD (3); LM-WM. |
| 2 | 71 | M | SR/PCC 90% | PDAC 10% | SRe | H | 2.5 | T2N2M0 | III | Yes | Yes | R1 (rp) | DO (2) |
| 3 | 76 | F | SR/PCC 90% | PDAC 10% | SRe | H | 4.2 | T3N2M0 | III | Yes | Yes | R1 (rp) | DD (2); LM-WM |
| 4 | 78 | F | SR/PCC 90% | PDAC 10% | SRe | H | 3.0 | T2N2M0 | III | Yes | Yes | R1 (rp) | AF (4) |
| 5 | 60 | F | SR 80% | PDAC 20% | SRe | H | 3.6 | T2N2M0 | III | Yes | Yes | R0 | DD (2); LM-WM |
| 6 | 74 | F | SR/PCC 80% | PDAC 20% | SRe | H | 0.6 | T1bN1M0 | IIB | Yes | Yes | R0 | DO (2) |
| 7 | 51 | F | SR 80% | PDAC 20% | SRe | H | 2.5 | T2N0M0 | IB | Yes | Yes | R0 | DD (18); LM, PC |
| 8 | 80 | F | SR/PCC 80% | PDAC 20% | SRe | H | 2.5 | T2N2M0 | III | Yes | Yes | R1 (rp) | AD (3); LM |
| 9 | 69 | M | SR/PCC 80% | PDAC 20% | SRe | H | 2.9 | T2N1M0 | IIB | Yes | Yes | R0 | NA |
| 10 | 66 | M | SR 80% | CA 20% | SRe | H | 2.1 | T2N1M0 | IIB | Yes | Yes | R0 | AF (5) |
| 11 | 77 | F | SR 80% | CA 20% | SRe | H | 1.5 | T1cN1M0 | IIB | Yes | Yes | R0 | NA |
| 12 | 77 | M | SR/PCC 60% | PDAC 40% | SRe | H | 3.0 | T2N2M0 | III | Yes | Yes | R0 | AD (8); LM, PC, SD |
| 13 | 72 | M | SR 60% | PDAC 40% | SRe | H | 1.6 | T1cN2M0 | III | Yes | Yes | R0 | DO (2) |
| 14 | 63 | F | SR 50% | PDAC 50% | SRe | T | 3.7 | T2N1M0 | IIB | Yes | Yes | R0 | AD (13); LM |
| 15 | 56 | M | SR 50% | PDAC 50% | SRe | H | 2.2 | T2N1M0 | IIB | Yes | Yes | R0 | AF (53) |
| 16 | 69 | M | SR/PCC 50% | PDAC 50% | SRe | H | 3.7 | T2N2M0 | III | Yes | Yes | R0 | DD (30); LM, PC |
| 17 | 57 | F | SR/PCC 50% | IPMN-ATC 50% | SRe | H | 4.1 | T3N2M0 | III | Yes | Yes | R0 | NA |
| 18 | 56 | M | SR 80% | PDAC 20% | Bi | B | 9.0 | T4NXM0 | III | Yes | No | NA | DD (8), NOS |
| 19 | 77 | F | SR 80% | PDAC 20% | Bi | H | 3.1 | T4N1M0 | III | Yes | No | NA | DD (7), NOS |
| 20 | 78 | M | SR 50% | PDAC 50% | Bi | T | 6.0 | T4NxM1 | IV | Yes | Yes | NA | DD (2), NOS |

AD, alive with disease; AF, alive free of disease; AUT, autopsy; B, body; Bi, biopsy; CA, colloid aspects; D, systemic dissemination; DD, dead of disease; DO, dead for other causes, surgical complications; H, pancreatic head; H-B, pancreatic head-body; IPMN-ATC, IPMN-associated tubular adenocarcinoma; LM, lung metastasis; LM-WM, lung metastasis followed <1 month by widespread metastasization; LVI, lympho-vascular invasion; NA, not available; NOS, not otherwise specifiable; PC, peritoneal carcinosis; PCC, poorly cohesive cells; PDAC, pancreatic ductal adenocarcinoma; PNI, perineural invasion; rp, retroperitoneal margin; SR, signet-ring cells; SRe, surgical resection; T, tail.

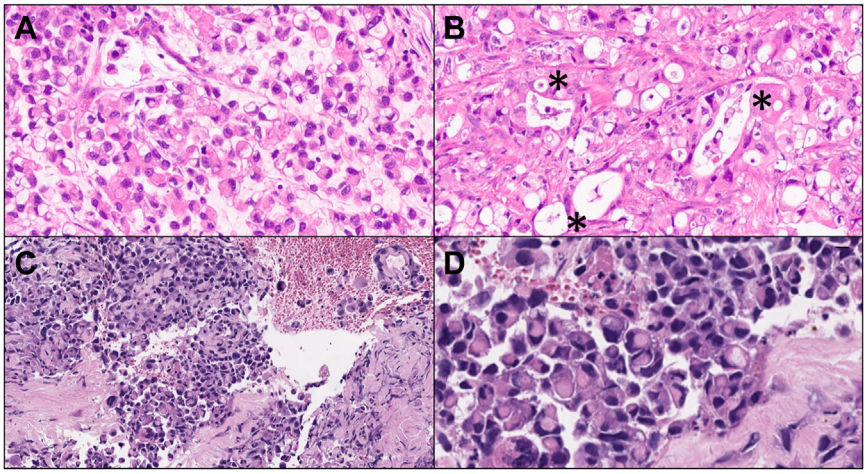


**Figure 1.**
Illustrative representations of pancreatic cancer with signet-ring/poorly cohesive cells (SRC): this cancer variant can be totally composed of SRC (A, hematoxylin and eosin, original magnification: 20×) or can show SRC in admixture with infiltrative glands (asterisks) (B, hematoxylin and eosin, 20×). Illustrative representations of material from fine-needle biopsy are also provided (hematoxylin and eosin, C 4×, D 40×).

*Molecular Analysis*

*Genomic Next-Generation Sequencing*

The pathogenic and likely pathogenic genetic alterations and copy number variations are summarized in Table 2, whereas variants of uncertain significance are reported in Supplementary Table S2. At genomic NGS, the cases exhibited a profile similar to that of conventional PDAC with the most common alterations affecting classical PDAC drivers. *KRAS* alterations were detected in 70% of cases, followed by *TP53* (55%), *SMAD4* (25%), and *CDKN2A* (20%). Recurrent somatic mutations were detected in *APC*, *NF1*, and *TGFBR2* (10% of each). Gene amplification represented a recurrent alteration. *KRAS* and *AKT2* were amplified in 2 different cases (10% each), and amplifications involving cyclin or cyclin-dependent kinase genes were also common (4 genes in total were amplified, including *CCNE1*, *CDK2*, *CDK4*, and *CDK6*). Homozygous deletions were detected in *CDKN2A* and *CDKN2B* (in the same 2 cases) and *EPHA3* (1 case).

Regarding potential targets for precision oncology, 4 cases displayed potentially actionable alterations. One case possessed a concomitant mutation and amplification of *EGFR*, 1 case harbored a somatic *PTEN* mutation, 1 case harbored a *RET* (exon 12) :: *CCDC6* (exon 8) fusion, and another case exhibited the presence of MSI. In this case (case #15), NGS did not detect any genetic alterations affecting the MMR genes. The tumor mutational burden ranged from 1 to 19.4 mut/Mb, and the highest value was observed in MSI tumors. None of the patients possessed any *CDH1* mutations.

*MSI Analysis*

Regarding the 1 case with MSI (case #15), immunohistochemical analysis for MMR proteins revealed a concomitant loss of expression of MLH1 and PMS2 with a maintained expression of MSH2 and MSH6. Using pyrosequencing, the presence of *MLH1* promoter methylation was demonstrated (methylation of CpG islands was 24%). Together, these results indicated that the presence of MSI, in this case, was not caused by MMR gene mutations and was instead due to *MLH1* promoter methylation.

*Transcriptome Analysis by RNA Sequencing*

All surgically resected specimen and the autopsy case were subjected to this analysis, and 4 cases were ultimately excluded due to poor RNA quality (old cases). Thus, 13 cases were analyzed using RNAseq.

First, the transcriptome profiles of the tumors were obtained. These profiles were then expressed based on the tumor composition (>80% vs <80% SRC). To define differences between the 2 groups of >80% (9 samples) vs <80% (4 samples) SRC, we performed differential expression (DE) analysis on the 2 groups. Using an adjusted *P*-value cutoff of .05, the 2 groups appeared to be very similar with only 6 differentially expressed genes. In particular, 4 of these (*CORO7*, *NTNG1*, *CLUHP3*, and *DXL3*) were specifically upregulated in cases with SRC $\geq$ 80%, whereas only 2 (*XACT* and *USP6*) were specifically upregulated in cases with SRC < 80% (Supplementary Table S3A).

Next, due to the high levels of similarities between the 2 groups ($\geq$ 80% vs < 80% SRC), we performed unsupervised hierarchical clustering on all samples. First, we used the NbClust package to estimate the best number of clusters, and our results indicated 2 ($k$=2). We then applied the hybrid hierarchical $k$-means approach to construct a dendrogram illustrating the relationships between samples. Unsupervised consensus clustering was performed using ConsensusClusterPlus to verify the resulting associations between the samples. The resulting consensus matrix confirmed the associations obtained by principal component analysis and the dendrogram.

The 2 clusters that were obtained included cluster A (CLA) comprised of 5 samples and cluster B (CLB) comprised 8 samples (Fig. 2). DE analysis between CLA and CLB identified 382 DE genes: 280 of these were enriched in CLA and 102 were enriched in CLB (Supplementary Table S3B). Of these, highly characterizing genes of CLA included genes of the exocrine pancreas such as genes encoding carboxypeptidases (*CPA1*, *CPA2*, and *CPB1*) and serine proteases (*PRSS*-genes). In contrast, highly characterized genes of CLB included genes encoding for different types of keratins (*KRT13*, *KRT17*, *KRT16P3*, and *KRT19*) and kallikrein (*KLK1*, *KLK6*, *KLK8*, and *KLK10*) (Fig. 3A).

Based on these results, using gene set enrichment analysis (GSEA) we analyzed different biological processes at the base of each cluster (Supplementary Figure S2). In particular, GSEA confirmed the predominance of biological processes linked to pancreatic metabolism in CLA, including adipogenesis and digestion, and to keratinization and epithelial to mesenchymal transition (EMT) signature in CLB (Supplementary Figure S2).

**Table 2**
Summary of pathogenic and likely pathogenic genetic mutations and CNV

| Patient ID | TMB | MSI | Gene variations | | | | | CNV | | | |
|---|---|---|---|---|---|---|---|---|---|---|---|
| | | | Gene | Variation | Mutation type | Frequency | Class | Gene | Variation | Copies | Class |
| 1 | 5.0 | No | *APC* | p.T1556fs*3 | Insertion – Frameshift | 16 | 5 | *RET*::*CCDC6* | CCDC6_ex8-RET_ex12 (Fusion product) | | |
| 2 | 7.8 | No | *KRAS* | p.G12D | Substitution – missense | 40 | 5 | *CDKN2A* | Hom Del exon 1 | | |
| | | | *TP53* | p.Q167* | Substitution – fonsense | 44 | 5 | *CDKN2B* | Hom Del exon 1 | | |
| | | | *CDKN2A* | p.Y44fs*76 | Insertion – frameshift | 34 | 4 | *FGFR1* | Gain | 4 | |
| | | | | | | | | *APLNR* | Gain | 4 | |
| | | | | | | | | *CDKN1B* | LOH | | |
| | | | | | | | | *EZH2* | LOH | | |
| 3 | 9.4 | No | *SMAD4* | p.G386S | Substitution – missense | 28 | 5 | Not identified | | | |
| | | | *SMAD4* | p.G419W | Substitution – missense | 17 | 4 | | | | |
| | | | *APC* | p.C2123* | Substitution – nonsense | 20 | 4 | | | | |
| | | | *NF1* | c.4111-1G>A | Substitution – splice acceptor | 15 | 4 | | | | |
| | | | *PTEN* | p.C83fs*17 | Insertion – frameshift | 41 | 4 | | | | |
| | | | *STK11* | p.L282fs*3 | Insertion – frameshift | 16 | 4 | | | | |
| 4 | 2.2 | No | *SMAD4* | p.G270fs*66 | Deletion – frameshift | 5 | 4 | Not identified | | | |
| 5 | 10.0 | No | *KRAS* | p.G12D | Substitution – missense | 27 | 5 | *PDGFRB* | Amp | 5 | 5 |
| | | | *TP53* | p.P151S | Substitution – missense | 31 | 5 | *EPHA3* | Hom Del | | 3 |
| | | | *SMAD4* | p.R445* | Substitution – nonsense | 28 | 5 | | | | |
| 6 | 6.1 | No | *TP53* | p.Q165* | Substitution – nonsense | 20 | 5 | *KRAS* | Amp | 54 | 5 |
| 7 | 1.0 | No | *BRCA2* | p.I2068fs*10 | Insertion – frameshift | 46 | 5 | Not identified | | | |
| 8 | 7.2 | No | *KRAS* | p.G12R | Substitution – missense | 18 | 5 | *AKT2* | Amp | 12 | 5 |
| | | | *TP53* | p.D281E | Substitution – missense | 32 | 5 | *CCNE1* | Gain | 4 | |
| | | | *CDKN2A* | p.T93fs*26 | Deletion – frameshift | 29 | 4 | *NF1* | LOH | | |
| | | | | | | | | *RNF43* | LOH | | |
| | | | | | | | | *TP53* | LOH | | |
| 9 | 9.4 | No | *KRAS* | p.G12V | Substitution – missense | 33 | 5 | *CDKN2A* | Disruptive SV | | |
| | | | *TP53* | p.F134fs*16 | Insertion – frameshift | 29 | 5 | | | | |
| 10 | 5.0 | No | | | | | | *CDK6* | Amp | 85 | 5 |
| | | | | | | | | *MDM2* | Amp | 37 | 5 |
| 11 | 8.3 | No | *KRAS* | p.G12R | Substitution – missense | 14 | 5 | Not identified | | | |
| | | | *TP53* | p.Q192* | Substitution – missense | 17 | 5 | | | | |
| 12 | 8.3 | No | *KRAS* | p.G12D | Substitution – missense | 21 | 5 | *CDK4* | Amp | 9 | 5 |
| | | | *TP53* | p.D259V | Substitution – missense | 25 | 5 | *CDK2* | Amp | 6 | 3 |
| | | | | | | | | *ETV6* | Amp | 14 | 3 |
| | | | | | | | | *SMAD4* | LOH | | |
| 13 | 5.6 | No | *KRAS* | p.G12V | Substitution – missense | 8 | 5 | Not identified | | | |
| | | | *SMAD4* | p.Q442* | Substitution – nonsense | 11 | 4 | | | | |
| 14 | 6.1 | No | *EGFR* | p.E746_A750del | Deletion – inframe | 59 | 5 | *EGFR* | Amp | 26 | 5 |
| | | | *TP53* | p.R175L | Substitution – missense | 12 | 5 | *B2M* | LOH | | |
| | | | | | | | | *TP53* | LOH | | |
| | | | | | | | | *RB1* | Del ex3-ex6 | | |
| 15 | 19.4 | Yes | *KRAS* | p.G13D | Substitution – missense | 12 | 5 | Not identified | | | |
| | | | *ERBB3* | p.V104M | Substitution – missense | 13 | 5 | | | | |
| | | | *NF1* | p.L898P | Substitution – missense | 15 | 5 | | | | |
| | | | *NF1* | p.I679fs*21 | Insertion – frameshift | 11 | 5 | | | | |
| | | | *TGFBR2* | p.K128fs*3 | Deletion – frameshift | 15 | 5 | | | | |
| | | | *ERBB3* | p.R667S | Substitution – missense | 12 | 4 | | | | |
| | | | *NF1* | p.C1939fs*19 | Deletion – frameshift | 7 | 4 | | | | |
| 16 | 8.9 | No | *KRAS* | p.G12D | Substitution – missense | 15 | 5 | Not identified | | | |
| | | | *TP53* | p.Q104* | Substitution – nonsense | 21 | 5 | | | | |
| 17 | 8.3 | No | *KRAS* | p.G12V | Substitution – missense | 32 | 5 | *CDKN2A* | Hom Del | | 5 |
| | | | *ATM* | p.V1268* | Deletion – frameshift | 38 | 5 | *CDKN2B* | Hom Del | | 5 |
| | | | *GNAS* | p.R201C | Substitution – missense | 24 | 5 | | | | |
| | | | *TGFBR2* | p.P129fs*3 | Insertion – frameshift | 31 | 4 | | | | |
| 18 | 7.2 | No | *KRAS* | p.G12D | Substitution – missense | 12 | 5 | Not identified | | | |
| 19 | 4.4 | No | *KRAS* | p.G12V | Substitution – missense | 54 | 5 | *CCNE1* | Amp | 38 | 5 |
| | | | *TP53* | p.P278S | Substitution – missense | 42 | 5 | *AKT2* | Amp | 27 | 5 |
| | | | | | | | | *KRAS* | Amp | 6 | 5 |
| 20 | 7.2 | No | *KRAS* | p.G12V | Substitution – missense | 33 | 5 | Not identified | | | |
| | | | *CDKN2A* | p.L78fs*41 | Deletion – frameshift | 40 | 5 | | | | |
| | | | *TP53* | p.R175H | Substitution – missense | 48 | 5 | | | | |
| | | | *SMAD4* | p.R497H | Substitution – missense | 35 | 5 | | | | |

TMB, tumor mutational burden; MSI, microsatellite instability; CNV, copy number variation; Amp, amplification; Hom Del, homozygous deletion; LOH, loss of heterozygosity.

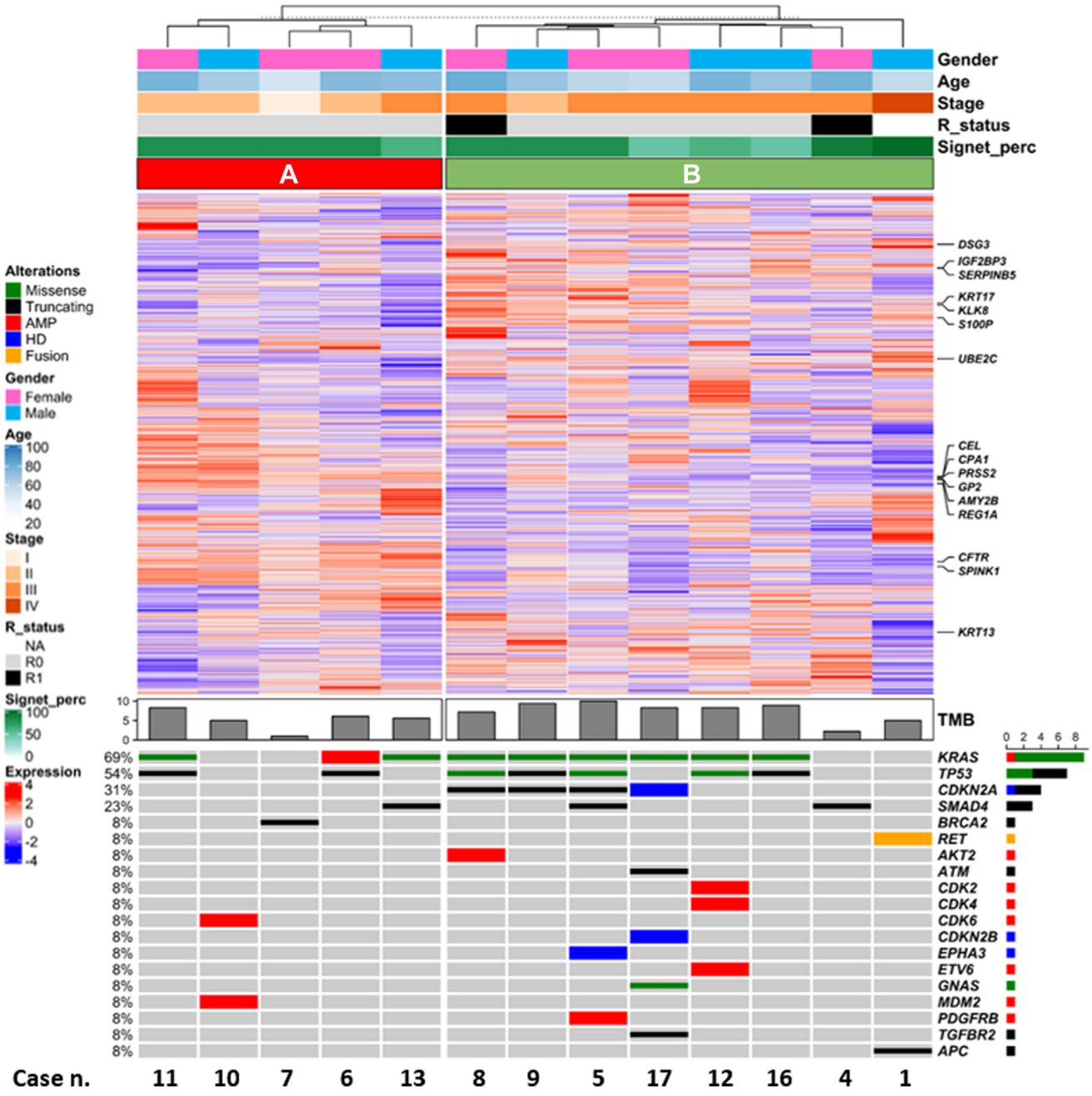


**Figure 2.**

Upper panel: gene expression heatmap stratified by the 2 consensus clusters (A and B) derived from the transcriptome analysis. Annotations for clinicopathologic variables are also provided. Lower panel: genomic alterations for essential tumor-related genes found in such clusters.

The comparison between the expression profile of each cluster and current PDAC classifiers highlighted that CLA was similar to the classic-pancreatic subtype and was associated with Moffitt et al's exocrine and Collisson's exocrine-like profiles, while CLB was similar to the squamous subtype and was associated with Bailey's squamous, Collisson's quasi-mesenchymal, and Moffitt's basal-like profiles (Fig. 3B). Regarding the additional Deseq2 algorithm and the coupled GSEA-based analysis for investigating differentially expressed genes between cases with and without lung metastasization, no statistically significant differences emerged between those groups of cases (all genes set: $P > .05$, Benjamini–Hochberg test).

*Additional Immunohistochemistry*

The results of additional IHC are summarized in Supplementary Table S4. The most commonly expressed mucin was MUC6, which was positive in 11/17 cases (64.7%); it also showed the highest mean value of the IHC combined score. Then, we specifically extracted the results of transcriptome analysis, plotting as a heatmap the expression of mucins-genes (Supplementary Figure S3). The comparison of the transcriptome with IHC showed a linear correspondence between the 2 analyses, with positive cases at IHC showing positive values on gene expression profiles, and vice versa. There were no differences in terms of mucins-genes expression between clusters A and B.

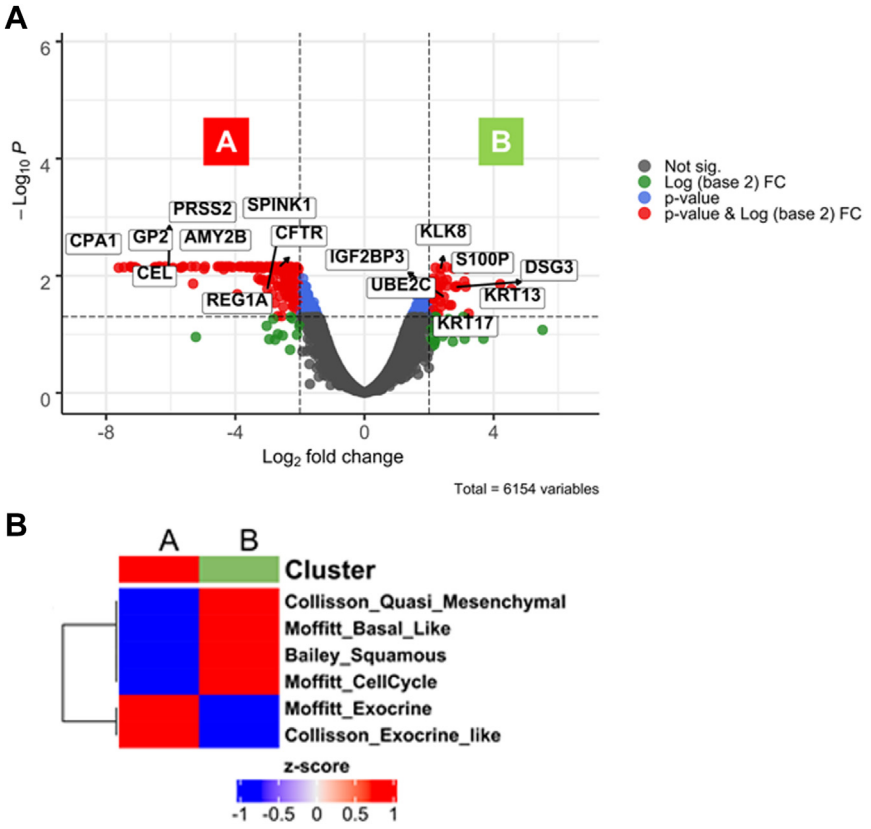


**Figure 3.**
Differential expression analysis between clusters A and B using the Deseq2 algorithm is here shown (A) and also expressed based on pancreatic signatures (B).

Regarding the analysis of cytokeratin 17 and 19, IHC validated the transcriptome findings. Indeed, all cases with squamous features, that is, the cases of cluster B, expressed both markers at IHC, whereas no cases of cluster A expressed these markers.

*Organoid-Based Analysis*

An explorative organoid culture was initiated from a resected tissue specimen of SRC-PDAC (Supplementary Figure S4A, B). Following the successful derivation of the cultures, organoids were embedded in paraffin for histopathologic evaluation. The main cytoarchitectural features of the parental tissue were retained (Supplementary Figure S4C, D). To understand if the organoid could replicate the same morphology in vivo, we transplanted immunodeficient mice with SRC-PDAC organoids. At the endpoint, tumor tissue was analyzed. SRC-PDAC histologically generated a tissue mirroring the parental one (Supplementary Figure S4E).

At the molecular level, the SRC-PDAC organoid presented with typical PDAC alterations, including somatic mutations in *KRAS and TP53* and also in *FBXW7* and *STK11* (Supplementary Figure S4F). The same genetic alterations were also identified in the parental tissues (Supplementary Figure S4F). Transcriptome analysis followed by molecular subtyping with GSVA revealed that the SRC-PDAC organoid (HCM-CSHL-0081-C25) could be classified as squamous according to the Bailey et al's classification.[24] and basal-like according to the classification proposed by Moffit et al.[26] (Supplementary Figure S4G). The primary conclusion was that SRC-PDAC organoids can be successfully generated and that SRC-PDAC cultures preserve the histologic and molecular features of SRC-PDAC tissues.

*Clinical/Survival Analysis*

*Study Population*

Overall, when considering only surgically resected patients and excluding those with unavailable follow-up data or those who died of surgical complications, a total of 10 PDAC with an SRC component were identified. Among them, 3 possessed a 50% SRC component, 1 possessed 60%, 4 possessed 80%, and 2 possessed 90% components. The control group included 480 patients with conventional PDAC (study flowchart in Supplementary Figure S5).

The median follow-up period of all cases was 50.2 months. The median DSS was 36.3 months (95% CI 32.5–41.0) with a median RFS of 16.6 months (95% CI 14.6–18.6). SRC was significantly associated with survival (HR 1.011, 95% CI 1.001–1.022, $P = .038$). The critical value of the SRC threshold for maximizing survival differences was 80%. Based on this threshold, the median DSS was 36.6 months (95% CI 32.7–41.3) vs 12.5 months (95% CI 2.0–NA) for patients with < and ≥ 80% SRC, respectively ($P < .001$) (Fig. 4A). Similarly, the median RFS was 16.8 months (95% CI 14.9–18.7) vs 4.5 months (95% CI 1.0–NA) for patients with < and ≥80% SRC, respectively ($P < .001$) (Fig. 4B).

For the multivariate analysis for DSS, the SRC component ≥80% remained statistically significant (HR 5.741, 95% CI 2.531–13.020, $P < .001$) together with tumor stage III vs I–II (HR 1.534, 95%

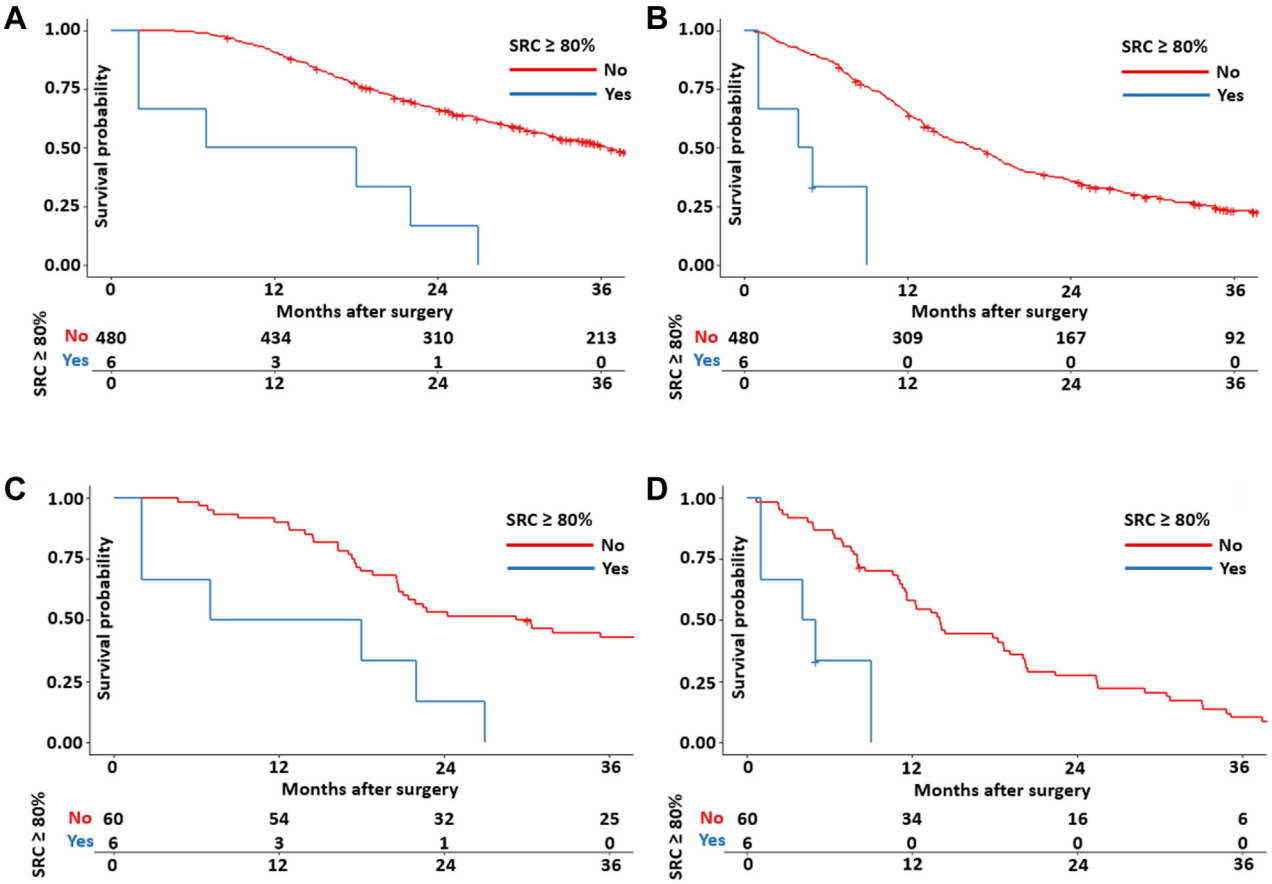


**Figure 4.**
Kaplan–Meier curves of pancreatic cancer with SRC ≥ 80% vs conventional pancreatic ductal adenocarcinoma (A: disease-specific survival; B: relapse-free survival), also analyzed with propensity score-matched analysis (C: disease-specific survival; D: relapse-free survival). SRC, signet-ring/poorly cohesive cells.

CI 1.219–1.931, $P < .001$). Upon multivariate analysis for RFS, SRC ≥ 80% remained statistically significant (HR 8.843, 95%CI 3.560–21.966, $P < .001$) together with tumor stage III vs I–II (HR 1.692, 95% CI 1.375–2.082, $P < .001$) and R1 vs R0 resection status (HR 1.302, 95% CI 1.058–1.604, $P = .012$). Regarding the survival analysis for genomic variables that was possible only in the cohort of pancreatic SRC, the mutational status of *KRAS* and *TP53*, and transcriptomic clusters were not statistically significant. *SMAD4* mutational status was associated with a poor prognosis and reached a statistically significant value for both DSS ($P = .025$) and RFS ($P = .025$).

As the SRC threshold of 80% was the most significant, for assessing the propensity-score matching we compared the SRC carcinomas satisfying this threshold (6 cases) to 60 conventional PDAC (matching 1:10, Supplementary Fig. S5) matched by age, sex, tumor stage, and R status. Propensity score-matched analysis confirmed the prognostic differences between ≥80% SRC carcinomas and conventional PDAC. The DSS of conventional and matched PDAC vs ≥80% SRC carcinomas was 29.8 (95% CI 21.0–47.9) vs 12.5 months (95% CI 2.0–NA), respectively ($P = .002$) (Fig. 4C). Similarly, RFS was significantly different between conventional and matched PDAC vs 80% SRC carcinomas at 14.0 (95% CI 11.6–20.1) vs 4.5 months (95%CI 1.0–NA), $P < .01$) (Fig. 4D). In the multivariate analysis, the presence of ≥ 80% SRC was the only independent predictor of DSS (HR 3.662, 95% CI 1.494–8.978, $P = .005$). Again, the ≥80% SRC component was independently associated with RFS in multivariate analysis (HR 8.521, 95% CI 2.922-24.852, $P < .001$) together with tumor stage III vs I–II for this survival index (HR 2.843, 95% CI 1.161–6.960, $P = .022$).

## Discussion

In this study, we provided clinicopathologic and molecular characterization of a series of pancreatic adenocarcinomas with SRC. First, we showed that SRC carcinomas are highly aggressive neoplasms, with the lungs as an elective metastatic site. Interestingly, an important prognostic driver was the SRC component: the higher this component, the poorer the prognosis. Furthermore, the genomic analysis showed that SRC carcinomas are similar to conventional PDAC, with the most common alterations affecting the classic PDAC drivers *KRAS*, *TP53*, *SMAD4*, and *CDKN2A*. Regarding actionable molecular targets, we reported the concomitant presence of mutation and amplification of *EGFR* (detected in the same case), the *RET*::*CCDC6* fusion gene, and MSI. The presence of *SMAD4* mutations was associated with poor prognosis. Transcriptome analysis showed that the cases clustered into 2 groups. Of them, 1 was enriched in genes associated with pancreatic metabolism and more similar to the classic/exocrine subtype, and the other one was enriched in genes linked with keratinization and EMT that was more similar to the squamous subtype. Also, we demonstrated that organoids from this specific PDAC variant can be successfully generated. Of note, their cultures preserve the histologic and molecular features of the parental SRC carcinoma.

One critical finding highlighted by the current study is the biological aggressiveness of such PDAC subtype, particularly for cases with SRC > 80%. This threshold is the one identified by the WHO classification as a diagnostic clue for this variant,[4] and our study is the first to demonstrate its clinical relevance, using 2 different validation cohorts. Interestingly, in gastric SRC a high proportion of SRC is typically associated with a better prognosis,[32] and this demonstrates the opposite biological significance of SRC in the pancreas. Of note, the clinical significance of the 80% threshold appears to be highly reliable, as it is derived by comparing the cohort of SRC carcinoma with 480 cases of conventional PDAC. Additionally, it has been further confirmed with a propensity score-matched analysis from a validation cohort of 60 patients with conventional PDAC. Another relevant clinicopathologic determination of this study is the presence of lung metastases as an elective site. This situation is uncommon for conventional PDAC, where cases with only lung metastasis are typically associated with a better prognosis.[33,34] In our series, although the lungs often appeared as the first metastatic site, in most cases, they were quickly followed by other disease localizations or widespread metastasis that ultimately resulted in a very poor prognosis.

Regarding the mutational landscape of pancreatic carcinoma with SRC, this histotype appears to be similar to conventional PDAC, as the classic PDAC drivers *KRAS*, *TP53*, *CDKN2A*, and *SMAD4* are the 4 most commonly altered genes. Interestingly, the prevalence of these alterations was slightly lower in this specific variant than in conventional PDAC.[35,36] The genetic similarities of PDAC variants to conventional PDAC, as also observed in our study, further confirm that the genomic profile alone cannot explain the peculiar morphology of the different PDAC histotypes.[37–40] An additional molecular approach comparing the SRC with the matched non-SRC component may be addressed by future studies. It would be of interest to study clonal evolution of SRC carcinoma and possible molecular drivers toward the acquisition of SRC morphology. Notably, we also reported the presence of 3 potentially actionable alterations in our cohort. The first is regarding the presence (in the same case) of *EGFR* mutation and amplification. *EGFR* alterations represent one of the most important actionable targets in non–small-cell lung cancer.[41,42] Moreover and specifically regarding *EGFR* amplification, a recent study reported significant benefits in terms of the overall survival of patients with *EGFR*-amplified gastroesophageal cancers treated with targeted therapy.[43] Based on our study, such biomarkers should also be assessed in SRC pancreatic cancer, as they could also represent a potential drug target in the pancreas.[44] Of note, in the case we reported, the lack of a co-occurring *KRAS* mutation renders this patient potentially eligible for EGFR inhibitors. An even more important clinical impact is provided by *RET* fusion and MSI, as these molecular alterations currently represent agnostic biomarkers for molecularly based treatments.[45,46] *RET* fusions are extremely rare events in pancreatic cancers, and the majority have been reported in specific subtypes such as acinar cells and ITPN-derived carcinomas.[47,48] MSI is a rare event in PDAC and is typically associated with medullary and colloid variants.[39] Based on the current study, SRC pancreatic cancer may also be potentially associated with these molecular alterations. Globally, in contrast to conventional PDAC and most PDAC variants.[6,7] pancreatic tumors with SRC, independently from SRC percentage, appear to be enriched in potential molecular targets (3/20 cases, 15%, a non-negligible percentage in pancreatic cancer). Thus, the possibility of performing high-throughput sequencing of selected cases with this morphology should be considered.

Another consideration of the mutational profile of SRC pancreatic cancer is the clinical impact of *SMAD4* mutations in our cohort. Previous studies have demonstrated that *SMAD4*-mutated PDAC is more often associated with a widespread metastatic pattern.[49] However, its mutational status was not correlated with survival in patients with conventional PDAC.[50] Based on our preliminary findings, *SMAD4* may serve as a prognostic biomarker in SRC; however, further studies are required to confirm this finding. The last consideration of the mutational landscape of SRC pancreatic cancer reported in this study is that in the pancreas, the *CDH1* gene is not a genetic driver beyond SRC morphology as it is in gastric cancer. This finding further corroborates the hypothesis that context matters regarding oncogenesis and tumor progression and that the tissue of origin is one of the most important factors influencing not only the molecular landscape but also the histomorphology of solid cancers.[51] Indeed, beyond similar morphology, the molecular background of pancreatic cancer with SRC appears to be completely different from that of gastric cancer with SRC.

Transcriptome analysis indicated that pancreatic SRC did not exhibit a common gene expression profile in all cases. They clustered into 2 groups, where one was more similar to the classic subtype and the other more similar to the squamous subtype. In particular, the group more similar to the classic subtype was enriched in genes associated with pancreatic metabolism, and this finding was also reported for pancreatic acinar cell carcinoma.[24] Conversely, the group that was more similar to the squamous subgroup was enriched in genes linked with keratinization and EMT. This distinction was further validated by specific IHC analysis with cytokeratin 17 and 19, which were specifically expressed only in the squamous cluster. Although we did not observe survival differences based on transcriptome profiles in our cohort, the second group may exhibit a more aggressive behavior, as in PDAC the presence of squamous features and the activation of EMT have been typically associated with a poorer prognosis.[24–26,52] Although a recent study on conventional PDAC showed different immune drivers related to different sites of tumor recurrence, including upregulation of neutrophilic markers in cases with lung metastasis,[53] we did not find any statistically significant difference in terms of gene expression profiles between cases with and without lung metastasis. This may be due to the small sample size, as well as to the biological peculiarities of SRC carcinoma. Regarding SRC carcinoma-derived organoids, we demonstrated for the first time the feasibility of obtaining organoids from this tumor type. Moreover, they appeared to retain the most significant cytoarchitectural features of the parental tissue in contrast to organoids obtained from conventional PDAC that typically form cystic structures as previously described.[54]

Our study does possess some limitations. First, DNA analysis did not investigate the entire genome of the lesions, and thus, potentially significant molecular events may have been missed. Nonetheless, the CORE panel we adopted was based on previously reported whole-genome sequencing that focused on clinically relevant alterations. In addition, we did not compare the molecular profile of SRC cancers with the matched non-SRC component. This specific analysis may be of interest for a better understanding of the clonal evolution of these neoplasms and should be taken into account by future studies on this topic. Furthermore, the sample size of SRC pancreatic cancers in our study may have been relatively small, and this is particularly true for survival analysis, with only 6 cases >80% SRC included in this analysis. However, this represents the largest series of this PDAC variant in the literature, and the multicenter design we adopted provides a concrete

answer to the difficulties of collecting large case series of rare neoplasms.

In conclusion, in this study, we provided an integrative clinicopathologic and molecular characterization of a series of SRC pancreatic cancers. Although this tumor subgroup shares the most important genetic drivers with conventional PDAC, it also exhibits important peculiarities. These include the lungs as an elective metastatic site, the clinical relevance of the threshold of 80% SRC, and the enrichment of potential targets for precision oncology. Thus, in the context of PDAC, the correct identification of SRC variant is important given the distinctive clinicopathologic and genomic features and the clinical implications.

### *Author Contributions*

C.L. contributed toward conception and design; M.S., N.S., G.M., A.M., L.M., A.C., V.C., R.T.L., A.S., and C.L. conducted data analysis and interpretation; M.S., N.S., G.M., A.S., C.L. contributed to manuscript writing; all authors are responsible for the provision of study materials or patients, collection and assembling of data, and gave final approval of the manuscript, and are accountable for all aspects of the work.

### *Data Availability*

All data/information are available in the manuscript and the supplementary material.

### *Funding*

This study is supported by Associazione Italiana Ricerca sul Cancro (AIRC IG n. 26343); Fondazione Cariverona: Oncology Biobank Project "Antonio Schiavi" (prot. 203885/2017); Fondazione Italiana Malattie Pancreas (FIMP-Ministero Salute J38D190006-90001); Italian Ministry of Health (RF CO-2019-12369662: CUP: B39C21000370001); and personal university-funds for research (FUR Luchini, Verona University). VC is supported by Associazione Italiana Ricerca sul Cancro (AIRC grant no. 18178), EU (MSCA project PRECODE, grant no. 861196), and the National Cancer Institute (NCI, HHSN26100008).

### *Declaration of Competing Interest*

Nicola Silvestris has the following disclosure: Consulting or Advisory Role: SERVIER, Roche; Sara Lonardi has the following disclosure: (1) Consulting or Advisory Role: Amgen, AstraZeneca, Bristol-Myers Squibb, Daiichi Sankyo, Incyte, Lilly, Merck Serono, Mirati Therapeutics, MSD, SERVIER; (2) Speakers' Bureau: Amgen, Bristol-Myers Squibb, GlaxoSmithKline, Lilly, Merck Serono, Mirati, Therapeutics, MSD Oncology, Pierre Fabre, Roche, Servier; and (3) Research Funding: Amgen, AstraZeneca (Inst), Bayer (Inst), Bristol-Myers Squibb (Inst), Lilly (Inst), Merck Serono, Roche (Inst). The other authors declare no potential conflicts of interest.

### *Ethics Approval and Consent to Participate*

This study was approved by the Bari Ethics Committee (date of approval: October 1, 2018, project no. 242, code: 708/CE). Experiments involving organoids and clinical data extraction were approved by the Verona Ethics Committee (date of approval: September 19, 2018, project no. 1911, code: 61413, and PAD_R no. 1101 CESC).

## Supplementary Material

The online version contains supplementary material available at https://doi.org/10.1016/j.modpat.2023.100251

## References

1. Bray F, Ferlay J, Soerjomataram I, Siegel RL, Torre LA, Jemal A. Global cancer statistics 2018: GLOBOCAN estimates of incidence and mortality worldwide for 36 cancers in 185 countries. *CA Cancer J Clin*. 2018;68(6):394–424. https://doi.org/10.3322/caac.21492
2. Rahib L, Smith BD, Aizenberg R, Rosenzweig AB, Fleshman JM, Matrisian LM. Projecting cancer incidence and deaths to 2030: the unexpected burden of thyroid, liver, and pancreas cancers in the United States. *Cancer Res*. 2014;74(11):2913–2921. https://doi.org/10.1158/0008-5472.CAN-14-0155
3. Siegel RL, Miller KD, Wagle NS, Jemal A. Cancer statistics, 2023. *CA Cancer J Clin*. 2023;73(1):17–48. https://doi.org/10.3322/caac.21763
4. WHO Classification of Tumours Editorial Board. *Digestive system tumours*. Lyon: International Agency for Research on Cancer; 2019.
5. Herbst B, Zheng L. Precision medicine in pancreatic cancer: treating every patient as an exception. *Lancet Gastroenterol Hepatol*. 2019;4(10):805–810. https://doi.org/10.1016/S2468-1253(19)30175-X
6. Luchini C, Capelli P, Scarpa A. Pancreatic ductal adenocarcinoma and its variants. *Surg Pathol Clin*. 2016;9(4):547–560. https://doi.org/10.1016/j.path.2016.05.003
7. Bazzichetto C, Luchini C, Conciatori F, et al. Morphologic and molecular landscape of pancreatic cancer variants as the basis of new therapeutic strategies for precision oncology. *Int J Mol Sci*. 2020;21(22):8841. https://doi.org/10.3390/ijms21228841
8. Schawkat K, Manning MA, Glickman JN, Mortele KJ. Pancreatic ductal adenocarcinoma and its variants: pearls and perils. *Radiographics*. 2020;40:1219–1239. https://doi.org/10.1148/rg.2020190184
9. Tracey KJ, O'Brien MJ, Williams LF, et al. Signet ring carcinoma of the pancreas, a rare variant with very high CEA values. Immunohistologic comparison with adenocarcinoma. *Dig Dis Sci*. 1984;29:573–576. https://doi.org/10.1007/BF01296277
10. Terada T. Primary signet-ring cell carcinoma of the pancreas diagnosed by endoscopic retrograde pancreatic duct biopsy: a case report with an immunohistochemical study. *Endoscopy*. 2012;44S:E141–E142. https://doi.org/10.1055/s-0030-1257045
11. Caranti A, Budini M, Mangano M, Cirstaudi A, Demagistri D. Primary signet ring cell carcinoma of the pancreas. A case report about an extremely rare variant of pancreatic carcinoma. *Ann Ital Chir*. 2020;9:S2239253X2003443X. PMID 33427204.
12. Campbell DJ, Isch EL, Kozak GM, Yeo CJ. Primary pancreatic signet ring cell carcinoma: a case report and review of the literature. *J Pancreat Cancer*. 2021;7:1–7. https://doi.org/10.1089/pancan.2020.0013
13. Brunetti O, Luchini C, Argentiero A, et al. The Italian rare pancreatic exocrine cancer initiative. *Tumori*. 2019;105:353–358. https://doi.org/10.1177/0300891619839461
14. Mafficini A, Lawlor RT, Ghimenton C, et al. Solid pseudopapillary neoplasm of the pancreas and abdominal desmoid tumor in a patient carrying two different BRCA2 germline mutations: new horizons from tumor molecular profiling. *Genes*. 2021;12:481. https://doi.org/10.3390/genes12040481
15. Li H, Durbin R. Fast and accurate short read alignment with Burrows–Wheeler transform. *Bioinformatics*. 2014;25:1754–1760. https://doi.org/10.1093/bioinformatics/btp324
16. Tischler G, Leonard S. biobambam: tools for read pair collation based algorithms on BAM files. *Source Code Biol. Med*. 2014;9:13. https://doi.org/10.1186/1751-0473-9-13
17. Li H, Handsaker B, Wysoker A, et al. The sequence alignment/map format and SAMtools. *Bioinformatics*. 2009;25:2078–2079. https://doi.org/10.1093/bioinformatics/btp352
18. Papke DJ, Nowak JA, Yurgelun MB, et al. Validation of a targeted next-generation sequencing approach to detect mismatch repair deficiency in colorectal adenocarcinoma. *Mod Pathol*. 2018;31:1882–1890. https://doi.org/10.1038/s41379-018-0091-x
19. Ahdesmäki MJ, Chapman BA, Cingolani P, et al. Prioritisation of structural variant calls in cancer genomes. *PeerJ*. 2017;5:e3166. https://doi.org/10.7717/peerj.3166
20. Richards S, Aziz N, Bale S, et al. Standards and guidelines for the interpretation of sequence variants: a joint consensus recommendation of the American College of Medical Genetics and Genomics and the Association for

Molecular Pathology. *Genet Med*. 2015;17:405–423. https://doi.org/10.1038/gim.2015.30
21. Sciammarella C, Bencivenga M, Mafficini A, et al. Molecular analysis of an intestinal neuroendocrine/non-neuroendocrine neoplasm (MiNEN) reveals MLH1 methylation-driven microsatellite instability and a monoclonal origin: diagnostic and clinical implications. *Appl Immunohistochem Mol Morphol*. 2022;30:145–152. https://doi.org/10.1097/PAI.0000000000000969
22. Love MI, Huber W, Anders S. Moderated estimation of fold change and dispersion for RNA-seq data with DESeq2. *Genome Biol*. 2014;15:550. https://doi.org/10.1186/s13059-014-0550-8
23. Gu Z, Eils R, Schlesner M. Complex heatmaps reveal patterns and correlations in multidimensional genomic data. *Bioinformatics*. 2016;32:2847–2849. https://doi.org/10.1093/bioinformatics/btw313
24. Bailey P, Chang DK, Nones K, et al. Genomic analyses identify molecular subtypes of pancreatic cancer. *Nature*. 2016;531:47–52. https://doi.org/10.1038/nature16965
25. Collisson EA, Bailey P, Chang DK, Biankin AV. Molecular subtypes of pancreatic cancer. *Nat Rev Gastroenterol Hepatol*. 2019;16(4):207–220. https://doi.org/10.1038/s41575-019-0109-y
26. Moffitt RA, Marayati R, Flate EL, et al. Virtual microdissection identifies distinct tumor- and stroma-specific subtypes of pancreatic ductal adenocarcinoma. *Nat Genet*. 2015;47(10):1168–1178. https://doi.org/10.1038/ng.3398
27. Subramanian A, Tamayo P, Mootha VK, et al. Gene set enrichment analysis: a knowledge-based approach for interpreting genome-wide expression profiles. *Proc Natl Acad Sci USA*. 2005;102(43):15545–15550. https://doi.org/10.1073/pnas.0506580102
28. Liberzon A, Subramanian A, Pinchback R, Thorvaldsdóttir H, Tamayo P, Mesirov JP. Molecular signatures database (MSigDB) 3.0. *Bioinformatics*. 2011;27:1739–1740. https://doi.org/10.1093/bioinformatics/btr260
29. Luo W, Friedman MS, Shedden K, Hankenson KD, Woolf PJ. GAGE: generally applicable gene set enrichment for pathway analysis. *BMC Bioinformatics*. 2009;10:161. https://doi.org/10.1186/1471-2105-10-161
30. Luchini C, Parcesepe P, Nottegar A, et al. CD71 in gestational pathology: a versatile immunohistochemical marker with new possible applications. *Appl Immunohistochem Mol Morphol*. 2016;24(3):215–220. https://doi.org/10.1097/PAI.0000000000000175
31. Mattiolo P, Hong SM, Paolino G, et al. CD117 is a specific marker of intraductal papillary mucinous neoplasms (IPMN) of the pancreas, oncocytic subtype. *Int J Mol Sci*. 2020;21:5794. https://doi.org/10.3390/ijms21165794
32. Bencivenga M, Treppiedi E, Dal Cero M, et al. The amount of signet ring cells is significantly associated with tumour stage and survival in gastric poorly cohesive tumours. *J Surg Oncol*. 2020;121(7):1084–1089. https://doi.org/10.1002/jso.25885
33. Downs-Canner S, Zenati M, Boone BA, et al. The indolent nature of pulmonary metastases from ductal adenocarcinoma of the pancreas. *J Surg Oncol*. 2015;112(1):80–85. https://doi.org/10.1002/jso.23943
34. Arnaoutakis GJ, Rangachari D, Laheru DA, et al. Pulmonary resection for isolated pancreatic adenocarcinoma metastasis: an analysis of outcomes and survival. *J Gastrointest Surg*. 2011;15:1611–1617.
35. Jones S, Zhang X, Parsons DW, et al. Core signaling pathways in human pancreatic cancers revealed by global genomic analyses. *Science*. 2008;321(5897):1801–1806. https://doi.org/10.1126/science.1164368
36. Waddell N, Pajic M, Patch AM, et al. Whole genomes redefine the mutational landscape of pancreatic cancer. *Nature*. 2015;518(7540):495–501. https://doi.org/10.1038/nature14169
37. Luchini C, Pea A, Lionheart G, et al. Pancreatic undifferentiated carcinoma with osteoclast-like giant cells is genetically similar to, but clinically distinct from, conventional ductal adenocarcinoma. *J Pathol*. 2017;243:148–154. https://doi.org/10.1002/path.4941
38. Gkountakos A, Mafficini A, Lou E, et al. Genomic characterization of undifferentiated sarcomatoid carcinoma of the pancreas. *Hum Pathol*. 2022;128:124–133. https://doi.org/10.1016/j.humpath.2022.07.011
39. Luchini C, Brosens LAA, Wood LD, et al. Comprehensive characterisation of pancreatic ductal adenocarcinoma with microsatellite instability: histology, molecular pathology and clinical implications. *Gut*. 2021;70:148–156. https://doi.org/10.1002/path.4941
40. Fang Y, Su Z, Xie J, et al. Genomic signatures of pancreatic adenosquamous carcinoma (PASC). *J Pathol*. 2017;243:155–159. https://doi.org/10.1002/path.4943
41. Greenhalgh J, Boland A, Bates V, et al. First-line treatment of advanced epidermal growth factor receptor (EGFR) mutation positive non-squamous non-small cell lung cancer. *Cochrane Database Syst Rev*. 2021;3:CD010383. https://doi.org/10.1002/14651858.CD010383.pub2
42. Lee HJ, Jeong GH, Li H, et al. Efficacy and safety of epidermal growth factor receptor-tyrosine kinase inhibitor (EGFR-TKI) monotherapy for advanced EGFR-mutated non-small cell lung cancer: systematic review and meta-analysis. *Eur Rev Med Pharmacol Sci*. 2021;25:6232–6244. https://doi.org/10.26355/eurrev_202110_26993
43. Maron SB, Moya S, Morano F, et al. Epidermal growth factor receptor inhibition in epidermal growth factor receptor-amplified gastroesophageal cancer: retrospective global experience. *J Clin Oncol*. 2022;40:2458–2467. https://doi.org/10.1200/JCO.21.02453
44. Mateo J, Chakravarty D, Dienstmann R, et al. A framework to rank genomic alterations as targets for cancer precision medicine: the ESMO scale for clinical actionability of molecular targets (ESCAT). *Ann Oncol*. 2018;29:1895–1902. https://doi.org/10.1093/annonc/mdy263
45. Subbiah V, Wolf J, Konda B, et al. Tumour-agnostic efficacy and safety of selpercatinib in patients with RET fusion-positive solid tumours other than lung or thyroid tumours (LIBRETTO-001): a phase 1/2, open-label, basket trial. *Lancet Oncol*. 2022;23(10):1261–1273. https://doi.org/10.1016/S1470-2045(22)00541-1
46. Yoshino T, Pentheroudakis G, Mishima S, et al. JSCO-ESMO-ASCO-JSMO-TOS: international expert consensus recommendations for tumour-agnostic treatments in patients with solid tumours with microsatellite instability or NTRK fusions. *Ann Oncol*. 2020;31:861–872. https://doi.org/10.1016/j.annonc.2020.03.299
47. Chou A, Brown IS, Kumarasinghe MP, et al. RET gene rearrangements occur in a subset of pancreatic acinar cell carcinomas. *Mod Pathol*. 2020;33(4):657–664. https://doi.org/10.1038/s41379-019-0373-y
48. Mafficini A, Simbolo M, Shibata T, et al. Integrative characterization of intraductal tubulopapillary neoplasm (ITPN) of the pancreas and associated invasive adenocarcinoma. *Mod Pathol*. 2022;35(12):1929–1943. https://doi.org/10.1038/s41379-022-01143-2
49. Iacobuzio-Donahue CA, Fu B, et al. DPC4 gene status of the primary carcinoma correlates with patterns of failure in patients with pancreatic cancer. *J Clin Oncol*. 2009;27(11):1806–1813. https://doi.org/10.1200/JCO.2008.17.7188
50. Herman JM, Jabbour SK, Lin SH, et al. Smad4 loss correlates with higher rates of local and distant failure in pancreatic adenocarcinoma patients receiving adjuvant chemoradiation. *Pancreas*. 2018;47(2):208–212. https://doi.org/10.1097/MPA.0000000000000985
51. Schneider G, Schmidt-Supprian M, Rad R, Saur D. Tissue-specific tumorigenesis: context matters. *Nat Rev Cancer*. 2017;17(4):239–253. https://doi.org/10.1038/nrc.2017.5
52. Lawlor RT, Veronese N, Nottegar A, et al. Prognostic role of high-grade tumor budding in pancreatic ductal adenocarcinoma: a systematic review and meta-analysis with a focus on epithelial to mesenchymal transition. *Cancers (Basel)*. 2019;11:113. https://doi.org/10.3390/cancers11010113
53. Karamitopoulou E, Wenning AS, Acharjee A, et al. Spatially restricted tumour-associated and host-associated immune drivers correlate with the recurrence sites of pancreatic cancer. *Gut*. [Preprint. Posted online February 15, 2023]. https://doi.org/10.1136/gutjnl-2022-329371
54. Boj SF, Hwang CI, Baker LA, et al. Organoid models of human and mouse ductal pancreatic cancer. *Cell*. 2015;160:324–338. https://doi.org/10.1016/j.cell.2014.12.021